

Chapter 2

Materials and Methods

2.1 LCA Modelling Methods

In the current study, an attributional LCA approach was applied. As indicated in the introduction, LCA is a systems analysis approach, assessing the environmental aspects and impacts of product or service systems over their whole life cycle in accordance with the stated goal and scope of the study. Based on the initial unit processes and associated definitions in study scope, the LCI concerned with data collection and calculation procedures is conducted. In conjunction with LCI, the LCIA phase provides a systematic characterisation of the environmental and resource issues for the systems. In the LCIA phase, LCI results are assigned to impact categories and based on the category indicator selected, the indicator result for each impact category is calculated. Then, the conclusions drawn from the findings of LCA are identified, qualified, and evaluated in the interpretation phase, in relation to the aims declared in the goal and scope of study.

Definition of the goal and scope is therefore the basis for all LCA studies. In this chapter the goal and scope for the LCA research presented in this thesis are set out together with discussion of specific aspects of the data development undertaken in order to address this scope. The other phases of LCA are presented in [Chaps. 3–7](#).

2.1.1 Goal of LCA Study

The LCA research set out to explore the environmental attributes of using starch-based foams (primarily WBF) as alternatives to conventional petrochemical foam materials. A variety of product systems were examined to determine whether a ‘generic’ set of LCA conclusions could be established for starch-based foams and their comparison with petrochemical alternatives or whether the outcomes were

specific to the individual product systems and comparisons being studied. These goals were addressed through the following objectives:

- To determine the environmental profile of the production of starch-based foam derived from a specific variety of winter wheat (Soisson).
- To assess the environmental profiles of WBF in case studies representing the packaging, display and construction industries.
- To compare environmental burdens of WBF with those of ‘conventional’ petroleum-based foams made from EPS/HDPE/LDPE in the case studies.
- To model and compare diverse end-of-life scenarios for WBF.
- To explore two additional starch-based foams derived from potato and maize starches (PSBF/MSBF).

2.1.2 Scope of Study

2.1.2.1 Function of Product System and the Functional Unit

Case studies were developed for four product systems. Amongst the product systems modelled, WBF cool-box has been tested in the lab and through commercial trials and has been verified as a marketable product in the short-term; the other three products were potential products at lab-test stage and are simulated as concept products in the LCA modelling. Their function and functional units are defined below.

Insulated Corrugated Box

This case study modelled a corrugated-board box insulated with WBF (density 25 kg/m³) or PE foam (density 35 kg/m³) designed to provide packaging and a degree of thermal insulation for shipping of temperature sensitive products (*e.g.* perishable foods, pharmaceuticals).

The functional unit was: “a single 8.5 l capacity corrugated box insulated with WBF or PE foam to maintain a temperature below 5 °C for 24 h for the transport of temperature-sensitive contents (see Fig. 2.1)”.

Display Board

Conventional HDPE display boards are used for outdoor or indoor display purposes, such as posters, bulletins or advertisements. In this case study, conventional HDPE display boards with a 20 % recycled content and WBF concept products were compared.

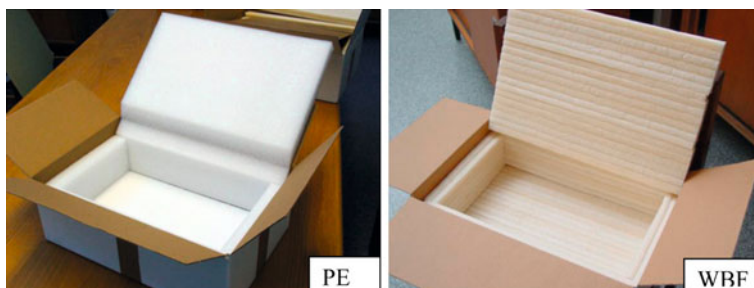


Fig. 2.1 PE coolbox (Hydropac Ltd. UK) vs. WBF coolbox (prototype)

Fig. 2.2 EPS trough mould
[18]



The functional unit was “a single display board used for indoor advertisement application with 2 m² surface area, 10 mm thickness and 3-month service life (excludes the artwork on the film rolled on to the board)”.

Trough Mould

As shown in Fig. 2.2, conventional reusable trough mould products manufactured by bonding PP skin to solid EPS core are used as a void-formers for constructing in situ ribbed concrete floor [18]. Generally after construction, the EPS trough moulds are left in situ for less than 6 months and then disposed, so in environmental terms they have medium-term life cycle. This design provides a cost efficient method to reduce concrete volume used and achieve longer spans than flat slabs.

Various grades of EPS with different density and compressive characteristics are used in trough moulds depending on the depth and side slope of the trough. Five case studies were conducted to compare WBF and two EPS grades (under trade name Filcor 20[®] and Filcor 45[®]), both of which contain recycled-EPS (30 and 15 % respectively) and have density of 15 and 20 kg/m³ respectively.

The functional unit was “EPS/WBF used as a specified trough mould core to deliver equal physical property and provide 6-month service life.”

Concrete Formwork

EPS foams are applied as formwork to construct simple or complex geometric structures such as spiral staircases, shaped columns, or external curved structures [17]. Generally EPS derived from virgin material are precisely cut off-site to provide a template for on-site concrete casting, but it has short life cycle—after a single use, they are disposed. Some EPS former products are lined with a coating to achieve a smooth surface. In this LCA study, Refractory lining and an EPS formwork for the ‘Doha Villa’ were modelled to compare virgin EPS (trade name Filcor 70®) and WBF used as short-life-cycle construction products. The functional units of the 2 case studies were:

A dome-shape single-use refractory former with 2.4 m³ volume, made from virgin EPS (density 25 kg/m³) or WBF (density 70 kg/m³)

A special-shape single-use formwork for the Doha Villa with a supplied volume of 335 m³ (approx an area of 670 m² and an average depth of 500 mm) made from virgin EPS or WBF.

2.1.2.2 Product System and System Boundary

The product system and unit processes presented here are those which are general to the life cycle of WBF in the case studies; the detailed unit processes specific to an individual, life-cycle-phase are presented in subsequent chapters.

The generic product system for WBF products is illustrated as Fig. 2.3. The following unit processes are considered within the system boundary: production of wheat grain, flour milling, and production of WBF production of the finished products using the WBF (the insulated cardboard boxes, display boards, trough moulds and refractory formers), distribution, end-of-life and transportation.

The inputs/outputs for the product system(s) included raw/ancillary material inputs, process energy input, other inputs and final or intermediate products, co-products, by-products, emission to atmosphere, water, and land. Environmental burdens associated with land use and human labour were excluded from the system boundary.

Unit processes either producing the inputs (*e.g.* production and delivery of process energy) or receiving the outputs (*e.g.* recycling of waste paper) were also included, but in some circumstances not every input and output can be modelled [49]. The criteria used to include inflows and outflows in the study were:

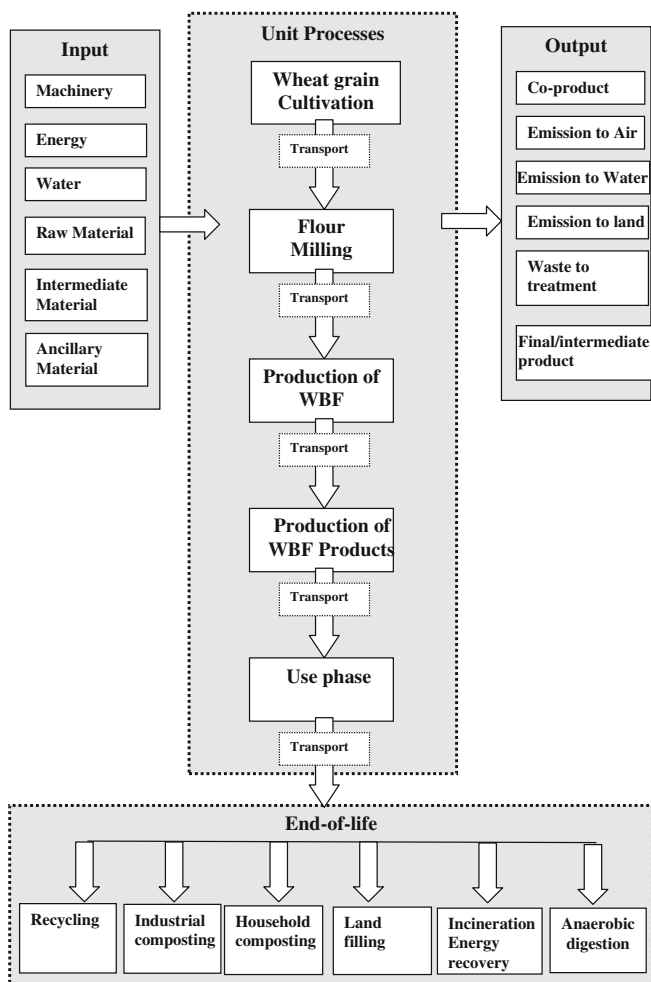


Fig. 2.3 Diagram for WBF products life cycle

- Data availability for the given input or output. Data were not available for all the inputs/outputs—these are defined as missing data. Such missing data are listed below, and their potential significance was considered in the sensitivity analysis and the interpretation phase.
- No specific cut-off rule (*e.g.* 2 % by mass) was applied. Instead, during the LCI development as much relevant data as possible for the product systems were sought and it is estimated that approximately 95–98 % of the mass and energy flow for all systems was achieved.

Based on these criteria, the following material/aspects were omitted:

- Energy consumption, infrastructure and other inputs in conversion of HDPE/WBF block to display board.
- Energy consumption, infrastructure and other inputs in conversion of EPS/WBF block to trough moulds and refractory former.
- The same artwork printing technology for WBF and HDPE display boards were assumed, so the production of artwork-film rolled on to the display boards were not included in system boundary.
- The same skin/coating materials for WBF and EPS trough moulds/concrete former were assumed, therefore, the production of skin/coating materials was not taken into account.
- The models for production of LDPE/HDPE/expandable PS were based on EU average data [10]. Some transportation operations are stated to be omitted from the Plastics Europe database [11].

Besides, infrastructure was another concern. Although the effects of these components on the products they produce are usually negligible due to the large throughput achieved in their lifetime, the environmental impacts of capital plant and buildings could be high. Thus the baseline approach in the current study was to include infrastructure, its exclusion was explored in the sensitivity analysis. Surrogate processes for infrastructure were applied for the production of WBF and its end-of-life.

2.1.2.3 Allocation Procedures

Several industrial processes in the present study yield more than one product (multi-output system) and, therefore, an allocation procedure needs to be applied so that upstream environmental interventions and wastes can be correctly shared amongst these products. A number of methodological options exist for such allocation in LCA [49]. Briefly, these are (a) to avoid allocation by system expansion, (b) to partition the inputs and outputs either by physical relationship (i.e. mass etc.) or other relationship such as economic value [56]. As discussed in Sect. 1.3.1.2, the selection of allocation approaches for ALCA remains a controversial issue. Although the relevance of system boundary expansion to ALCA has been questioned by some LCA practitioners [102], in the current ALCA study system boundary expansion was applied in the cases where energy related co-products occurred (e.g. electricity from CHP, electricity from AD biogas) or closed-loop recycling occurred. This was based on the following considerations:

- 1) this approach is generally accepted to be relevant to ALCA and moreover is recommended as the preferred approach in PAS 2050 [14, 27].
- 2) for the energy co-products examined, hypothetical historical changes were investigated.

Besides, in this study, allocation by economic relationship (accounting for price and quantity) (except CO₂, see [Sect. 2.1.2.3](#)) was adopted for most of the stages where multiple-products occurred. Examples are discussed in detail below:

‘Avoided Burdens’ Approach for the Allocation of Co-Produced Energy from the CHP System and Bio-Gas Plant

The ‘avoided burdens’ approach, i.e. allocation by substitution [[56](#), [71](#)] was applied in the paper production processes and the end-of-life scenarios (landfill, AD, incineration). The surplus electricity produced in the CHP system and sold to the national grid [[25](#)] is a co-product of the paper/cardboard manufacturing process. In the case of waste treatment processes, including landfill, AD and incineration, electric and/or thermal energy are produced; electricity is sold to the national grid whereas thermal energy is wasted. In these processes, the inputs and outputs for the equivalent quantity of electrical power generated by the average electricity generation supply mix for the UK grid are allocated as a ‘credit’ to the modelled systems.

Allocation by Economic Value

Allocation by economic value was adopted for all inputs and outputs (except CO₂, see below) in the flour milling process according to the respective value and quantity of flour and its co-product (wheat feed). The same approach was applied to soy flour production process—the environmental burdens were allocated among the soy flour and soy oil based on the yield and price.

Carbon Counting

Economic value-based allocation was not adopted in accounting for the biogenic CO₂ inputs and biogenic carbon-based emissions in the life cycle because attempt to allocation carbon by economic value introduces serious distortions in the predicted carbon sequestration and release between main product(s) and co- and by-products. In order to ‘track’ the carbon footprint during the life cycle of WBFs, a stoichiometric carbon counting approach was applied to determine (1) carbon sequestration into the wheat flour component of the WBF (during the crop growth phase of the life cycle) and, (2) the downstream release of this carbon during subsequent processing, product use and final disposal stages of the life cycle. Based on the carbon content in wheat starch and protein, the carbon sequestered into the wheat flour used for WBF was calculated in terms of its CO₂ equivalents. The ‘sequestration’ of this amount of carbon during the crop growth phase of the life cycle thus represents a ‘negative’ GHG balance at this stage which is then returned to the environment in various ways dependant upon the subsequent ‘fate’

of the WBF product(s). This carbon-accounting approach enables clear recognition of the stages of the life cycle where GHG emissions are either mitigated or exacerbated and also facilitates identification of various options for enhancing GHG mitigation strategies.

Closed-Loop Allocation

The recycled EPS/PE/cardboard may be re-used within the same product system, or used in other product systems (recycled material undergoes changes in inherent properties, *e.g.* recycled EPS used as plastic wood). The former is referred to as “closed-loop recycling” the latter as “open-loop recycling”. In this study the close-loop allocation approach was applied—virgin material for the life cycle is assumed to be displaced by recycled material within the same product system.

2.1.2.4 Data Categories

The data categories applied in this study include:

- Raw material inputs, *e.g.* CO₂ from atmosphere, cooling or process water.
- Energy inputs or outputs such as electricity, natural gas, and heavy fuel oil (to calculate GJ from m³ or tonnes of fuel, the net calorific value published by DTI was used [22].
- Intermediate products: such as wheat grain, pesticides, NPK compound fertilizer, flour, corrugated board.
- Final products, such as insulated coolboxes with PE foam or WBF.
- Emissions to air water or land: CO₂, N₂O etc.
- Wastes to be treated *e.g.* paper rejects, wood waste to be recycled.

2.1.2.5 Data Quality Requirements

Data Quality Parameters

The three data quality parameters [51] used in this study are defined as:

- Time-related coverage: in this study the reference years are 2006–2008. Primary data collected from specific companies are no more than 5 year old prior to 2008. Secondary data from published sources are generally within 10 years prior to 2008.
- Geographical coverage: primary data has been collected from the site-specific manufacturers under study; for the secondary data, UK sources were preferred, if not available, EU or global data was used.

- Technology coverage: primary data was from defined processes from consultations and visits to manufacturing sites; secondary data have been collected from trade associations and government reports which are representative of the process. If neither was available, data from a different technology (surrogates) or laboratory scale (data development) was used.

Data Quality Indicators

The indicators to characterize the quality of the data used in this study are: (1) precision: a measure of the variability of data values for each data category; (2) completeness: indicated by the percentage of locations out of the total number in existence; (3) representativeness: an indicator of the degree to which the data set reflects the true measurement of the population of interest [51], it involves geographic, temporal and technological dimensions.

The quality and nature of data were characterised by both qualitative and quantitative aspects: the data sources were clarified and the uncertainty of either industry-based or literature-based data were analyzed by the method indicated in Sect. 2.3.2.

2.1.2.6 LCIA Methods

Two LCIA elements are concerned: characterisation and normalization. Characterisation is to assign and convert LCI results (unit process data); the numerical indicator results represent the characterisation outcome. Normalization aims to calculate the magnitude of the category indicator results relative to a reference baseline.

The impact categories, characterisation models and category indicators used are shown in Table 2.1.

Most of the models shown in Table 2.1 are incorporated in the CML 2 baseline 2000 V2.04 characterisation model [34], except IPCC AR4, instead, IPCC AR3 is included [28]. CML 2 baseline 2000 V2.04 adopts a problem oriented (midpoint) approach and is used in the current study as the 'default' LCIA method. However, a second LCIA method—Eco Indicator 99 (a damage-oriented approach) defining impact categories at the endpoint level was also applied to analyse the sensitivity of the LCIA results to the LCIA method choice.

As an optional LCIA element, normalization changes the outcome of the characterisation and gives a normalized LCIA profile for the product system [50]. The reference system provided by CML 2 baseline 2000 V2.04 West Europe 1995 was used as default method [80], but a second normalization method was applied in sensitivity analysis. In West Europe 1995, the total annual emission or resource

Table 2.1 Characterisation models

Impact category	Characterisation model	Category indicator	Indicator result	References
Eutrophication potential	Model based on stoichiometry procedure	Deposition increase divided by N/P equivalents in biomass	kg PO ₄ -equivalents	[38]
Acidification potential	RAINS model	Deposition/acidification critical load	kg SO ₂ equivalents	[46]
Ecotoxicity and human toxicity potential	USES-LCA model	Predicted environmental concentration increase/predicted no-effect concentration	kg 1,4- DB (1,4-dichlorobenzene) equivalents	[39, 42]
GWP100	IPCC model	Infrared radiative forcing (W/m ²)	kg of CO ₂ -equivalents	IPCC AR4 (fourth assessment report) [29]
POCP	Trajectory model	Quantity of tropospheric ozone formed	kg C ₂ H ₂ equivalents	[21, 52], [20]
ODP	Montreal protocol	Stratospheric ozone breakdown	kg CFC-11 equivalents	World meteorological organisation [105]

use in Western Europe for the given year 1995 are chosen as reference value. All of these reference values have been reported by Huijbregts et al. [40]. However, as pointed out by Heijungs et al. [37], biased normalization profiles can be delivered due to the limitations in the coverage of elemental flows for the product system and for the reference system. A large degree of bias may occur in normalized indicator results for impact categories which are not well-established (e.g. marine eco-toxicity, land use) or that are related to many substances (e.g. human and eco-toxicities). Particularly biased marine ecotoxic results have been observed [37]. Limitation in the characterization factors for toxicity-related impact categories have been discussed in previous studies [39, 42, 85]. It should be noted with regard to the present study that the USES-LCA model for metals is debatable and moreover that missing data and knowledge impose limitations on the toxicity models, especially for the marine eco-toxicity model where no experimental data were available.

2.2 Agro-Eco-System Modelling Methods

Since 1990 when the IPCC first assessment report was released, agriculture has been seen as an important source of GHGs. In addition to GWP, agriculture also contributes to other impact categories such as acidification and eutrophication potentials via leaching or trace gas emissions. To simulate the carbon and nitrogen biogeochemistry in agro-ecosystem, two approaches were applied in this study: the empirical model IPCC approach [62], and a process-oriented model DNDC (Denitrification-Decomposition).

2.2.1 IPCC Approach

To estimate the emissions from the agricultural system, such as N_2O emissions from soil, CO_2 from liming, IPCC tier 1 approaches [48] were applied. Here soil N_2O emission estimation is given as example. The IPCC method accounts for both direct and indirect N_2O emissions (both pathways are defined in IPCC Guidelines) [48]. It utilizes activity data and emission factors (EF) to derive the N_2O emission estimations to the level of N input [48].

However, the IPCC EFs are derived from field measurement at sites in a variety of countries with different soil types, climate and crops [13], and so have a wide range, leading to a large degree of uncertainty in the emission estimation [12]. Moreover, the IPCC Tier 1 methodology is intended to be broadly applicable rather than being site-specific, it does not account for regional difference in agro-ecosystem characteristics and should be regarded as a first approximation [44].

To estimate the combined uncertainty for the IPCC method-derived GHGs inventory, IPCC guidelines [48] established two approaches: Approach 1 uses a simple error propagation equation; whilst in Approach 2 Monte Carlo simulation is recommended. Monte Carlo Simulation is a computational algorithm method. In the Monte Carlo process, pseudo-random samples of inputs are generated by an algorithm (pseudo-random number generator) [48] from the probability density function (PDF) specified for each input variable; then one random value for each input is entered into the model to arrive at one estimate of the model output. After repeating this process for a number of iterations, multiple estimations representing the sample values from PDF of model output was obtained. By analyzing the samples of model output, the mean, SD (standard deviation), and 95 % confidence interval of output PDF can be inferred.

In this study, Approach 2 was adopted; uncertainties in EF were determined according to uncertainty ranges given in the IPCC Guidelines [48]. RiskAMP Monte Carlo Add-In Library version 2.97 (Professional Edition, Structured Data, LLC) statistical analysis software was used to perform the Monte Carlo simulation.

2.2.2 Process-Oriented Model DNDC

The process-oriented models take into account site-specific factors such as fertilizer type, climate, crop rotation, agricultural management. Described below is the rainfall event-driven process-based model used.

2.2.2.1 DNDC Model Structure

DNDC was selected for this LCA research and its latest version DNDC93 was modified and applied in this site specific study in the UK. DNDC bridges ecological drivers and soil biochemical reactions via linking both to soil environmental factors. In the DNDC model, classical laws of physics, chemistry and biology or empirical equations obtained from laboratory observation were used to parameterize geochemical/biochemical reactions [63, 64]. The original parameters and equations have been published in details [63–66].

The structure of DNDC is presented in Fig. 2.4. The DNDC model comprises two interacting components—the first includes 3 sub-models (soil climate, plant growth and decomposition) and predicts soil environmental variables based on ecological drivers; the second component consists of nitrification, denitrification and fermentation sub-models simulating microbial activity and trace gas fluxes and N leaching [64].

The six sub-models play different parts and interact with each other. The soil climate sub-model integrates climate, soil properties and O_2 profile to simulate soil temperature moisture and Eh [63, 65]. The climate, soil, crop parameters and field operations are integrated in the plant-growth sub-model to estimate crop growth, and its effects on soil temperature, moisture, available N and DOC etc. [66]. The decomposition sub-model mainly models 4 pools of soil organic carbon—microbial biomass, plant residues, active humus and passive humus; in addition, N dynamics during decomposition of organic matter in soil are simulated as well (e.g. nitrogen mineralized enters the inorganic nitrogen pool as NH_4^+ which is either nitrified to NO_3^- or is removed via crop-uptake, leaching or volatilization) [62, 63]. The denitrification sub-model is activated by increase in soil moisture or decrease in oxygen level from events like rainfall, flooding, and freezing temperatures (below $-5\text{ }^\circ\text{C}$) [62]; when these events occur, the production, consumption and diffusion of NO and N_2O are simulated. Another main source of NO and N_2O , nitrification is included as a sub-model in DNDC and nitrification-induced NO and N_2O is calculated as a function of predicted nitrification rate and temperature and is influenced by the soil environmental variables. In addition, the NH_4^+/NH_3 equilibrium and functions for NH_3 production and volatilization are also included in the nitrification model [63]. The release of CH_4 is modelled in a fermentation sub-model, where CH_4 production, oxidation, and transport under submerged conditions is calculated based on fermentation equations [63].

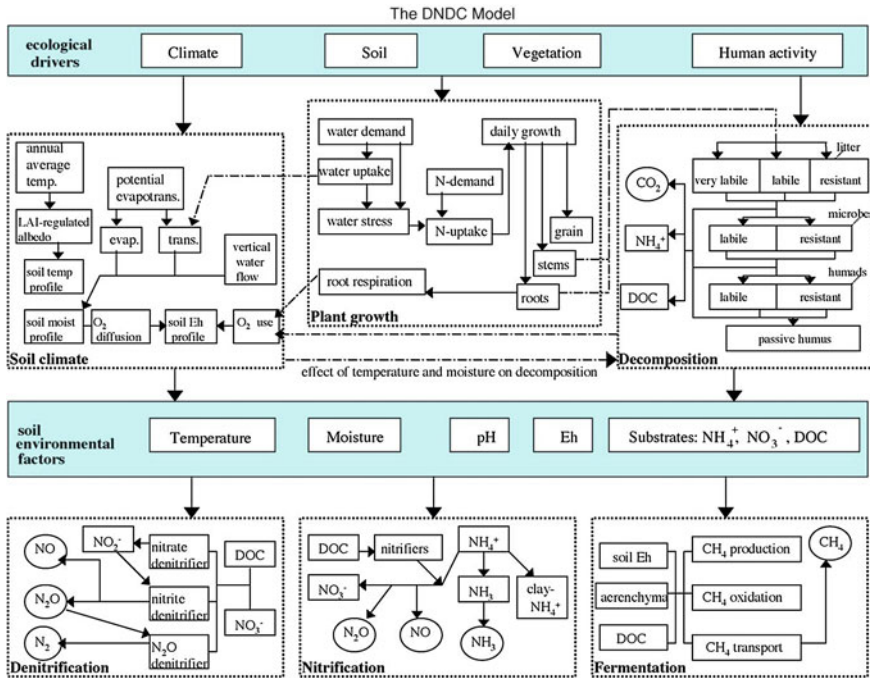


Fig. 2.4 Structure of DNDC model [64]

2.2.2.2 DNDC Input Data

The specific data on soil characteristics, daily climate, crops and farming practice for each of the 6 fields located in Norfolk that produced Soisson winter wheat for WBF manufacture were used as input to the DNDC model. The farming database for the six fields over five years (2003–2007) were obtained in collaboration with Heygates Farm Swaffham Ltd, whose cooperation is gratefully acknowledged.

The soil types and soil properties for the different soil layers at Swaffham farm were obtained based on the National Soil Map/Inventory and provided by the National Soil Research Institute (NSRI) of Cranfield University. This inventory covering over 50 % of arable land and grassland in England and Wales was developed from a soil survey conducted on the basis of a 5-km soil sampling grid. The specific research methods for this soil survey were reported by Bellamy et al. [7]. This soil map/inventory represents the most accurate comprehensive source of data on soil at the national level in the UK [74], and was used as the soil database for the UK-DNDC model [13]. According to this soil map, two soil associations (soil associations present a group of soil types which are typically found occurring together i.e. associated in the landscape) covering an area of 554 km² and accounting for 0.37 % of England and Wales's landmass are present in the Swaffham farm area and comprise multiple soil series(soil types). Soil texture was

identified based on a soil texture triangle [99] and the UK soil classification [73] and it together with the soil composition reported by Swaffham farm were applied in the DNDC.

Besides soil, another important ecological driver is climate. Daily meteorological data for the five year period 2003–2007 were collected from a weather station run by Broom's Barn, which is 30 miles away from the farm modelled. The data include daily maximum and minimum temperature ($^{\circ}\text{C}$), precipitation (mm) and wind speed (m/second).

Both NH_4^+ concentration in rainfall and atmospheric NH_3 concentration were derived from a database provided by the Centre of Ecology and Hydrology (CEH). Within UK National Ammonia Monitoring Network (NAMN) operated by CEH, there are 95 sites developed for exploration of concentration and deposition of $\text{NH}_3/\text{NH}_4^+$. Rainfall NH_4^+ concentration for the Swaffham farm area was estimated based on the 2006 UK map for ammonium ion rain concentration [15]. Atmospheric NH_3 concentration was calculated according to the data collected from a site (Stoke Ferry) closest to Swaffham farm (9.2 miles away) [16]. The sampling methods are described in CEH report [98].

As for the atmospheric CO_2 concentration and its annual increase rate, several data sources were considered and compared—CDIAC website (CO_2 Information Analysis Centre), study conducted by Reay et al. [83], IPCC as well as personal communication with Professor Keith Goulding from Rothamsted Research [32].

2.2.2.3 Sensitivity Analysis and Uncertainty Analysis for DNDC Outputs

Compared with climate data and farming practice, the soil properties are highly variable in spatial terms even within one single field. Averages of the soil survey data cannot solve this issue, as the correlation between modelled trace gas and any of the soil properties is non-linear in the DNDC model [67]. To test the sensitivity and uncertainty of the DNDC simulation to the variability of soil parameters, the following methods were adopted.

In sensitivity tests, a baseline scenario was constructed by using the mean value for soil characteristics, daily climate, crops and farming practice. Alternative scenarios were built up by varying each of the soil parameters across a range provided by NSRI. To quantify the sensitivity analysis and determine the most sensitive factors for modelling trace gas and leaching, a sensitive index [64] was introduced:

$$S = \frac{\left(\frac{O_2 - O_1}{O_{\text{avg}}} \right)}{\left(\frac{I_2 - I_1}{I_{\text{avg}}} \right)} \quad (2.1)$$

where S is the relative sensitivity index; I_1 , I_2 are the minimum and maximum input values for a given parameter; I_{avg} is the mean value of I_1 and I_2 . O_1 and O_2 are the model outputs corresponding to I_1 and I_2 . O_{avg} is the mean value of O_1 and O_2 . The

higher the absolute value of S , the greater the impact the input parameter has on the output. A negative value of S indicates an inverse relationship between input and output.

Based on the sensitivity analysis results, the two most sensitive soil parameters for each trace gas (N_2O , CH_4 , and NH_3) or N leaching were identified and then explored in uncertainty analysis. In this research, the methodology for Monte Carlo simulation in DNDC93 was modified in collaboration with the model originators at the University of New Hampshire. Originally, when DNDC was running in the Monte Carlo mode, the range defined for each ecological variable was divided into eight intervals fitting a discrete distribution. Then random samples were selected from the eight intervals and entered into the model. However, this only represents eight samples from the potential the range of inputs. In the modification of DNDC93 implemented here, the sample size was increased from 8 to 50. In other words, the range defined for each variable was divided into fifty intervals, and then the random sample generated within these 50 intervals was entered into the model. The Monte Carlo simulation was run with an iteration of 5,000. The 5,000 fluxes for trace gases based on the randomized soil parameters were generated and further analyzed by the methods described in the next section. A further modification was to the simulation period. The original DNDC93 did not allow users to define the time period for the outputs from Monte Carlo simulation, only the summary data for one year (365 Julian days) was provided. In the modified DNDC93 flexibility was increased so that the model outputs are given as total gas-flux/leaching for any user-defined period, which allowed uncertainty analysis of simulated results to be conducted based on a time boundary such as one wheat crop cycle which was more appropriate to the scope of this LCA.

2.2.2.4 Statistical Analysis of DNDC Results

In this statistical analysis, the simulated trace gas emissions and leaching from the DNDC model were the observed samples. They were fitted with various hypothesized standard distributions. The GOF of each distribution was assessed and from this analysis the best-fit distribution was selected.

This analysis starts with counting the frequency of the observed samples that falls into a range of equally-distributed intervals or bins. The frequency in each bin is the observed frequency O_i . After that, standard distributions are fitted to the observed samples. A widely used technique known as MLE is applied to assess the characteristic parameters θ_m of each distribution. This technique is frequently used for parameter estimation and fitting distribution to available dataset [97, 104]. Suppose the observed data X_1, \dots, X_n are independent and identically-distributed random variables with a common standard PDF $f(x_i; \theta)$. The likelihood function is defined as:

$$L(\theta; x) = \prod_{i=1}^n f(x_i; \theta), \quad \theta \in \Omega \quad (2.2)$$

where $x = (x_1, \dots, x_n)$ is the data of the observed sample. θ can be a scalar or a vector, depending on the PDF of the distribution. For instance, the θ for the PDF of the normal and lognormal distribution is a vector consisting of the mean and SD [97]. The maximum likelihood estimator θ_m is the parameter for the distribution that fits the observed sample best. It is the value of θ which maximizes the function $L(\theta)$, which is solved by differentiating the logarithm of $L(\theta; x)$ as follows:

$$\frac{\partial l(\theta)}{\partial \theta} = 0$$

where function

$$l(\theta) = \log L(\theta) = \sum_{i=1}^n \log f(x_i; \theta), \quad \theta \in \Omega \quad (2.3)$$

Sample size is one of the most important factors affecting the robustness of MLE. The larger the sample size, the smaller is the bias in the parameter estimates [8]. In this study, the sample size was 5,000. The PDF of the hypothesized distribution as a function of x was calculated by MLE and is expressed as $f(x; \theta_m)$. Using this method, the PDF of all distributions were calculated.

In order to identify the best fit distribution, the PDF of each hypothesized distribution was compared with the observed sample distribution of the results using GOF tests. Two non-parametric test methods were applied—the Chi square test and the Kolmogorov–Smirnov test (K–S test). Both address how well the observed samples conform to the hypothesized distributions expressed by a null hypothesis H_0 (i.e. no difference).

The Chi square test statistic is given as

$$\chi^2 = \sum_{i=1}^n (O_i - E_i)^2 / E_i \quad (2.4)$$

where n is number of bins; O_i is the observed frequency or number of counts in bin i , E_i is the expected frequency of the hypothesized distribution in bin i . Chi square is used as a measure of how far a sample distribution deviates from a hypothesized distribution; the larger the disagreement between the observed and the expected frequency, the larger is the χ^2 value obtained. Based on the degree of freedom df , defined as $n-1$, and the χ^2 value, tables for the critical values of the Chi square distribution indicate the probability p for the occurrence of a given χ^2 value if H_0 is true. If $p < \alpha$ (significance level, $\alpha = 0.05$ was applied here), then the null hypothesis is rejected.

The Chi squared test above was performed on all the distributions. After that, the χ^2 values were ranked. The distribution with the smallest χ^2 value is the best fit distribution for the observed samples.

The K–S test originally was developed for continuous data, and is more powerful than Chi square when the sample size is small [107]. It quantifies the maximum absolute deviation between cumulative empirical frequencies $F(x)$ and cumulative density function (cdf) for the hypothesized distribution $G(x)$. The test statistic is given as

$$d_{\max} = \sup_x |F(x) - G(x)| \quad (2.5)$$

where the data is grouped into bins; sup is the supremum of set of data $|F(x) - G(x)|$ for each bin. According to the total number of data, and the number of bins n , a critical value at significance level α ($\alpha = 0.05$ was applied) is given in the critical value table for the K–S test. If d_{\max} is greater than critical value, then H_0 is rejected. Using the K–S test critical value table, the probability p can be obtained. In addition, by the K–S test statistics d_{\max} for all the hypothesized distributions were ranked. The distribution with the lowest d_{\max} value is the best representative of the observed samples. In most situations, the best distributions identified by the two tests are the same. However, when discrepancy occurs, the distribution identified by the Chi square test takes priority as this test is suitable for the large sample size used in this analysis.

The statistical analysis was performed in Matlab in collaboration with Dennis Lee in the Civil and Environmental Engineering Department of Imperial College. The best-fitted distribution identified for the simulated DNDC results was used as input data for the uncertainty analysis of the LCA in Simapro 7 (v 7.1.8).

2.3 Sensitivity Analysis and Uncertainty Analysis of the LCA Results

This section presents the general methodologies for testing the sensitivity of the LCA results to different parameters (such as LCI results, characterisation models), and the uncertainty of LCA results due to the input uncertainty and variability in the LCI data.

2.3.1 Sensitivity Analysis

A series of sensitivity analyses were conducted to analyze the influence of a given parameter on the LCIA results including the characterisation and normalization models. The parameters assessed include unit process data, characterisation factors, allocation rules, system boundary, the omitted unit process and scenarios.

2.3.1.1 Tornado Diagram

Tornado Diagrams were used to assess the sensitivity of the results for one product system to data for a single unit process and to identify the most sensitive parameter [9, 100]. In this approach, the LCA model is run with the extreme values for one parameter while all other parameters are kept constant. The results are presented in bar graphs to indicate the degree to which the outputs vary due to the changes in individual parameters- the top bar represents the most sensitive parameter while the bottom bar shows the least sensitive one.

2.3.1.2 Scenario Sensitivity Analysis

In the case of other parameters, such as the characterisation model, allocation rules, and the system boundaries, sensitivity tests were conducted through scenarios. Here, the scenarios are defined as descriptions of possible future situations, based on specific future assumptions and they are characterised by the choice of parameters listed above [9]. A sensitivity test involves calculation based on all possible scenarios for the tested parameter(s) and analysis of the influences of the relevant parameter(s) on either the characterisation or normalization profiles or the comparison ranking. For one product system, 10 % changes in the characterised or normalized indicator results was chosen as the threshold above which the influences of parameter on the model results were considered to be significant.

2.3.2 Uncertainty Analysis

2.3.2.1 Uncertainty of the LCI Analysis

The uncertainty introduced into the LCI results due to the cumulative effects of input uncertainty and variability of inventory data were quantified by the following methods.

MLE and GOF Methods

In the case of an industry-based inventory data with multiple measurements or a computer-simulated inventory data with information on variability, statistical methods (MLE and GOF) were applied to fit the probability distribution to the observed or simulated data. The specific methodology is described in [Sect. 2.2.2.4](#) where distribution fitting for DNDC simulated data was given as an example.

Pedigree Matrix Method

For literature-based secondary data or industry-based primary data which were only represented as single measurement values, temporal, geographical, or technological gaps are the likely major sources of uncertainty. In such cases, MLE and GOF are not applicable and an expert judgement-based approach termed Pedigree Matrix was applied. The Pedigree Matrix approach was originally developed by Weidema and Wesnæs [103], and was adopted and modified in other studies to represent uncertainty in LCI data [9, 41, 59]. The Pedigree Matrix approach is also introduced in the Ecoinvent database [31], transforms the data quality indicators (such as completeness and representativeness) to probability distributions by representing the data quality indicator value by a 'default' lognormal distribution. Specifically, uncertainty in inventory data is characterised by six characteristics (from U_1 to U_6). Each characteristic is divided to five levels with a score (1–5), and an uncertainty factor in terms of contribution to the square of the geometric SD is given to each score of the six characteristics.

The geometric SD (at 95 % confidence interval) is defined as:

$$\sigma^2 = \exp \sqrt{[\ln(U_1)]^2 + [\ln(U_2)]^2 + [\ln(U_3)]^2 + [\ln(U_4)]^2 + [\ln(U_5)]^2 + [\ln(U_6)]^2 + [\ln(U_b)]^2} \quad (2.6)$$

where: U_1 is the uncertainty factor of reliability; U_2 is the uncertainty factor of completeness; U_3 is the uncertainty factor of temporal coverage; U_4 is the uncertainty factor of geographic coverage; U_5 is the uncertainty of technological coverage, U_6 is the uncertainty factor of sample size; U_b is the basic uncertainty factor which is based on expert judgement. The Pedigree Matrix defining criteria for data quality assessment and the uncertainty factors are given in Appendix A.

In this method, the 95 % confidence interval for each inventory datum was estimated based on the mean value μ and the SD σ^2 : (μ/σ^2 ; $\mu \times \sigma^2$) [1].

2.3.2.2 Uncertainty of LCIA Results

Statistical variability in LCI data or the lack of temporal, geographical or technological dimensions in the LCI introduces uncertainty in the LCIA results. As indicated before, uncertainty of LCI data is expressed as a probability distribution, either log-normal-distributed random errors introduced by the Pedigree Matrix method, or PDF identified by statistical methods. Based on these, Monte Carlo simulation was applied to estimate the uncertainties in the LCIA results.

Monte Carlo simulation was built in Simapro 7.0 software and it was run with 1,000 iterations at significance level $\alpha = 0.05$. By analyzing samples of the model output, the mean, SD, and 95 % confidence intervals of the output PDF are given as results of the uncertainty analysis.

2.4 Experimental Methods

The main test materials of interest in this LCA were WBF provided by Greenlight Products Ltd (plus cardboard box from Hydropac Ltd); and the additional potato/maize starch-based foams produced in Greenlight Ltd for comparison with WBF.

2.4.1 *Experimental Set-Up*

2.4.1.1 AD Inocula

The inocula were collected from a mesophilic (30–40 °C), wet (<15 % dry solid), continuous-feeding and multiple stage (hydrolysis step and methanogenesis stage) digestion system operated by a UK commercial AD plant. The operation temperature for the anaerobic digesters was 37 °C and OLR to digesters was variable due to the varying BFMSW composition; based on laboratory results by this UK commercial AD plant, the average OLR over 3 months (Jan 2009–March 2009) is 2.393 g COD/L/day with a coefficient of variation (CV) of 0.184.

2.4.1.2 BMP

The BMP assay was conducted according to the techniques developed by Owen et al. [75]. The media contain nutrients and vitamins for mixed anaerobic cultures [75] and Resazurin was added as an indicator to detect oxygen contamination (turns pink when oxidized). The BMP assay was run in 165 or 39 ml serum bottles fitted with leak proof Teflon seals and with controls of inoculum without substrate.

In each bottle, the total liquid volume of 100 or 20 ml was added (volumes for 165 and 39 ml serum bottle respectively), including media, inoculum and substrates. Anaerobic conditions were maintained during media and inoculum transfers by flushing the media flasks and assay bottles with a 70 %/30 % v/v mix of N₂/CO₂ at a flow rate of approx 0.5 L/min. Each serum bottle was then immediately capped with Teflon seals when the gas flushing needle was removed.

The inocula were taken from active BFMSW anaerobic digesters operated by a UK commercial AD plant (see 2.4.1.1). To deplete the residual biodegradable organic material present in inocula before the BMP test, they were pre-incubated in a 1 L batch reactor under anaerobic conditions at 30 °C until no significant CH₄ was produced. Then the pre-incubated inocula were used in the BMP assays to give a final concentration of 2 gVSS/L in the serum bottles.

To determine the inoculum activity, the protocol proposed by Angelidaki et al. [2] was applied. Model substrates chosen to determine hydrolytic, acidogenic, acetogenic and methanogenic activities were amorphous cellulose (1 g/L), glucose

(1 g/L), a mixture of propionic and butyric acid (0.5 g/L for each acid), and acetic acid (1 g/L) respectively.

The BMP assays for different substrates including foams and cardboards were conducted at an approximate 1:1 ratio of inoculum VSS to substrate COD [82]. All the serum bottles were incubated at 37 °C and shaken at 200 rpm in Gallenkamp Orbital Incubator.

Gas and liquid samples were collected to determine the composition of biogas and the concentration of VFAs. All controls and substrates were assayed in triplicate for gas composition analysis and the CVs for the three replicates were within 0.08; where VFA analysis was undertaken, four identical bottles were set up for each feeding, and one was used for VFAs measurements.

2.4.2 Analytical Methods

2.4.2.1 Gas Composition Analysis

In the BMP test, the volume of biogas produced in the serum bottle was determined by a glass syringe. A glass syringe lubricated with diH₂O and pre-flushed with the CO₂/N₂ (30 %/70 % v/v) gas mixture was used to determine the gas volumes produced in the serum bottle headspace. The volume reading was taken by allowing the syringe plunger to gently move and equilibrate between the bottle and room air pressure. After determining the volume, the syringe with biogas was removed.

To determine the composition of biogas, a 1 ml headspace gas sample was collected using a 1 ml plastic syringe (Terumo) and assayed in a gas chromatograph (Shimadzu GC-14A) equipped with thermal conductivity detector (TCD); a Porapak N column (1500 × 6.35 mm) was used for analysis. The carrier gas for GC analysis was helium set at a flow rate of 50 ml/min. The temperature of the column, detector and injection port were set at 28, 38 and 128 °C respectively. The peak areas and gas concentration readings were calculated and collected on a Shimadzu Chromatopac C-R6A integrator. Calibration gases were accurate to 5 % and the CV for 10 identical samples was 0.02. Ultimate CH₄ potential was expressed as the amount of yielded CH₄ (converted to standard temperature and pressure) divided by the quantity of VS and COD added.

2.4.2.2 Volatile Fatty Acids

After mixing samples well by inverting the serum bottles, 2 ml liquid samples were collected from the bottles using plastic syringes (through Teflon seals). These were then centrifuged at 13,000 rpm for 2 min and the supernatant was filtered through a

0.22 μm filter (VWR Labshop). 1 ml of the filtered sample was then transferred to GC vials, acidified by adding one drop of 98 % sulphuric acid and analyzed on the gas chromatograph (Shimadzu GC-2014) fitted with a flame-ionised detector (FID) and a SGE capillary column (BP21, 12 m \times 53 mm ID with film thickness 0.5 μm). The carrier gas was helium at a flow rate of 102.5 ml/min; the temperature for injector and detector were constant at 200 and 250 $^{\circ}\text{C}$ respectively; the initial temperature for the column was 80 $^{\circ}\text{C}$, then increasing by 10 $^{\circ}\text{C}/\text{min}$ to 160 $^{\circ}\text{C}$ after which the temperature was held for 1 min. The concentration for acetic, propionic, n-butyric, iso-butyric, n-valeric, iso-valeric and n-caproic acids were analyzed and the CV for ten identical samples was 0.066.

2.4.2.3 Element Sulphur Analysis

A three-step sequential microwave digestion by HNO_3 , H_2O_2 , and HCl and Inductive coupled Plasma (ICP) measurement developed by Kalra et al. [57] for multiple-element analysis of plant materials was used for S elemental determination. Unlike the HNO_3 - HClO_4 wet digestion which has been reported as a method with low recovery of S due to S-containing gases or incomplete oxidation of certain compounds [35, 108], this microwave digestion method in closed vessel could minimize S loss [93]. Furthermore, ICP is applicable to all soluble form of S.

1 g fresh foam/cardboard sample (with moisture content determined) was transferred into a digestion vessel to which 10 ml HNO_3 was added, the vessel was swirled gently to ensure all sample came into contact with HNO_3 . All vessels were loosely capped and placed in the microwave oven (Anton Paar Multiwave 3000). Samples were digested for 30 min at 540 W setting. After completion of the heating cycle, the vessels were cooled for 5 min, then a 1 ml H_2O_2 was added to each sample solution. Mixtures were kept at room temperature for over 5 min until the bubbling ceased. Then the digestion vessels were placed back into the oven and a second heating cycle at 540 W was run for 15 min. The digestion solutions were cooled down for 5 min before adding 2 ml HCl and returned back to oven. At the end of the final heating cycle (180 W 10 min), a clear solution was obtained. The sample solutions were filtered through filter paper (Whatman Grade No. 42) into a 50 ml volumetric flask. The vessels were rinsed with 1 M HCl for three times to ensure the materials were quantitatively transferred into the funnels. The filtration volume was made up to 50 ml. The sample was analyzed on ICP-OES (Inductive Coupled Plasma-Optical Emission Spectrometer) (Perkin Elmer Optima 7300DV). Argon was used as both carrier gas and purging gas (to remove interfering oxygen from the system). The detection limits for S is 30 $\mu\text{g}/\text{L}$ and the three emission lines used for sulphur were S I 180.669, 181.975, 182.563 nm.

A NaSO_4 standard was used for calibration and the recovery rates for S and the matrix interferences were tested by spiking the samples and blanks with NaSO_4 .

2.4.3 Physical–Chemical Methods

2.4.3.1 Total solid (TS), volatile solid (VS)

Total solid (TS) and volatile solid (VS) were assayed according to standard methods [3, 70, 88, 89]. The empty aluminium dishes were placed in a furnace at 550 °C for 1 h. After cooling in a desiccator, the sample was transferred into the pre-weighed dish, and placed in an oven at 103–105 °C for 24 h until achieving constant weight (constant weight is defined as less than ± 0.3 mg change in the weight upon one hour of re-heating). The resulting weight was recorded for the measurement of TS and then the dish was placed in a muffle furnace at 575 ± 25 °C for approximately 24 h. After cooling in a dessicator, the sample was weighed and then placed back in the muffle furnace at 575 ± 25 °C, and ashed to constant weight. VS content refers to the difference between the weight of a sample before and after ashing. The calculation was performed according to the following equations

$$\%TS = \frac{WEIGHT_{ovendrysample+dish} - WEIGHT_{dish}}{WEIGHT_{receivedsample}} \times 100 \quad (2.7)$$

$$\%VS \text{ of TS} = \frac{WEIGHT_{ovendrysample+dish} - WEIGHT_{ash+dish}}{WEIGHT_{receivedsample} \times \%TS/100} \times 100 \quad (2.8)$$

where

$WEIGHT_{dish}$

the weight of empty aluminium dish

$WEIGHT_{receivedsample}$

the weight of sample as received

$WEIGHT_{ovendrysample+dish}$

the weight of sample plus dish after oven drying

$WEIGHT_{ash+dish}$

the weight of sample plus dish after ashing in muffle furnace.

2.4.3.2 Total Suspended Solid, Volatile Suspended Solids

Total Suspended Solid (TSS) and Volatile Suspended Solids (VSS) were assayed according to standard methods [3]. Glass fibre filters were prepared for the assay by inserting them onto the base and clamping these into funnels. Under vacuum, the filters were washed with three successive 20 ml volumes of deionised water (diH_2O). All traces of water were removed by continuing to apply vacuum. The glass fibre filters were then placed in aluminum dishes and held in the muffle furnace at 575 ± 25 °C for 1 h. The filters were rewashed with three additional successive 20 ml deionised water aliquots, and dried in an oven at 103–105 °C for one hour. Then the dishes and filters were removed directly to the desiccator and cooled for use in VSS/TSS assays.

A prepared filter was placed on the base and clamped on a funnel. The filter was wetted with a small volume of deionised water to seal it against the base. Then a small amount of sample (0.1–0.25 ml) was transferred to the filter by pipette and the filter (with sample on it) was rinsed with diH₂O three times. All traces of water were removed under vacuum. The filter with sample was removed to the prepared aluminium dish and oven dried at 103–105 °C for 24 h. The mass of the sample was then determined and then was placed back to the oven until constant weight was achieved. Afterwards, the dish and filter were placed in the muffle furnace at 575 ± 25 °C overnight and directly removed to desiccator. After cooling, the sample mass was recorded and it was then returned to the furnace to ash to constant weight. VSS and TSS were calculated according to the following equations

$$\text{TSS(g/L)} = \frac{\text{WEIGHT}_{\text{ovendry}} - \text{WEIGHT}_{\text{dish+filter}}}{\text{Inoculum}} \quad (2.9)$$

$$\text{VSS(g/L)} = \frac{\text{WEIGHT}_{\text{ovendry}} - \text{WEIGHT}_{\text{ash}}}{\text{Inoculum}} \quad (2.10)$$

where

$\text{WEIGHT}_{\text{dish+filter}}$ the weight of empty aluminium dish and filter after oven drying

$\text{WEIGHT}_{\text{ovendry}}$ the weight of oven dried dish, filter plus residue

$\text{WEIGHT}_{\text{ash}}$ the weight of residue, dish and filter after ignition in muffle furnace

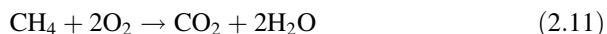
Inoculum (mL) the volume of inoculum filtered.

2.4.3.3 COD Measurements

The measurement of COD was based on the Standard Closed Reflux Colorimetric Method [3]. Digestion solutions were prepared by adding 10.216 g of K₂Cr₂O₇ (dried overnight at 103 °C), 167 ml of concentrated H₂SO₄ and 33.3 g of HgSO₄ into 500 ml of diH₂O. The mixture was then cooled at room temperature before diluting to 1,000 ml with diH₂O. 1 ml of the prepared sample was added to a Hatch reflux tube, followed by 0.6 ml of digestion solution. Then 1.4 ml of acidified silver sulphate reagent (2.5 % w/w Ag₂SO₄ in H₂SO₄) was carefully added to the tube so that an acid layer was formed under the digestion solution layer. After the tubes were sealed and inverted three times (to mix properly) they were refluxed in a Hach COD reflux reactor (Model 45600) at 150 °C for 2 h. After cooling to room temperature, the samples were analysed on a UV/VIS scanning spectrophotometer (Shimadzu Model UV-2101PC) at 600 nm wavelength. Solutions of potassium hydrogen phthalate (KHP with theoretical COD of 1.176 mg O₂/mg.) were used as standards for calibration.

Total COD (TCOD) was obtained by taking 50 mg of sample and diluting it to 50 ml with diH₂O. The presence of particles in suspension makes it difficult to take representative samples. All COD assays were performed in ten replicates. The CV for the replicate samples was within 0.12.

The calculation of theoretical CH₄ potential (COD equivalence of CH₄) was based on the following equation



Each mole of CH₄ consumes two moles of oxygen. Therefore, 1 g COD destruction is equivalent to 0.35L CH₄ at 0 °C and 760 mm Hg pressure (STP) or 0.395L CH₄ at 35 °C and one atmosphere [96].

2.4.3.4 Total N Measurements

The measurement of total nitrogen was conducted based on the Hach TN kit protocol (Hach Lange GmbH). A 5 mg sample was added to digestion tube and diluted with 0.5 ml diH₂O. An alkaline persulfate digestion converted all forms of nitrogen to nitrate. Sodium metabisulfite was added after the digestion to eliminate halogen oxide interferences. Nitrate reacts with chromotropic acid under strongly acidic conditions to form a yellow complex with an absorbance maximum at 410 nm. The total N was measured on a Shimadzu UV/VIS scanning spectrophotometer (Model UV-2101PC) against blank. Ammonium chloride was used as a standard. The detection limits are 10–150 mgN/L, and the CV for ten identical samples was 0.11.

2.4.3.5 PVOH Measurement

This method was used to determine the PVOH residue left in the serum bottles after the BMP assay. The PVOH sample provided by Greenlight Ltd was used as a standard; a standard PVOH calibration solution (0–20 mg/L) was prepared.

PVOH was determined by a colorimetric method based on formation of a PVOH-iodine-boric acid blue complex. The PVOH-iodine complex is a helix structure formed by the vinyl alcohol groups and iodine; this helix is further stabilized by boric acid through its linkage of OH groups [26, 54]. Only the concentration range from 0 to 20 mg PVOH/L falls within Beer's law behaviour and so all samples were prepared within this range [6, 26].

4 % Boric acid solution was prepared by dissolving 4 g boric acid crystals in 90 ml water, at approx 80 °C and then diluting solution to 100 ml (after cooling to room temperature). Iodine solution was prepared by adding 1.27 g iodine and 2.5 g of potassium iodide in 100 ml diH₂O to give final concentrations of 0.05 M I₂ and 0.15 M KI. 0.15 ml of sample was treated with 0.75 ml of 4 % boric acid solution and 0.15 ml of iodine solution in turn and mixed well after each addition.

The final solution was diluted to 2.5 ml and kept at 25 °C for 15 min and then its absorbance was measured at 690 nm on a UV/VIS scanning spectrophotometer (Shimadzu UV-2101PC) against a blank solution containing the same amounts of boric acid and iodine solution.

2.4.3.6 Total Protein Measurements

Total protein content was measured by using a total protein kit (Sigma, product codes TP0300 and L3540) which was based on the modified Lowry assay developed by Peterson [78]. 5–10 mg foam samples were added to a test tube and diluted to 1 ml with diH₂O and 1 ml of Lowry reagent was added to each tube and mixed well. After maintaining at room temperature for 20 min, 0.5 ml Folin and Clocalteu's phenol reagent was added to the tubes with rapid and immediate mixing, and then the samples were left at room temperature for a further 30 min to develop a purple colour. The samples were transferred from tubes to cuvettes and analyzed on a Shimadzu UV/VIS scanning spectrophotometer (Model UV-2101 PC) against a blank at wavelength 750 nm [78]. All the absorption readings were finished within 30 min to avoid inaccuracy caused by the gradual loss of colour (colour loss is approx 1 % per hour at 20 °C).

Bovine serum albumin (BSA) was used as a standard to determine calibration curves. The detection limit was 5 mg/L and the CV for ten identical samples was within 0.166.

Besides the determination of total protein present in WBF, this method was also applied to estimate the wheat protein residue left in the serum bottles after the BMP test. After mixing the samples, over 1 ml liquid samples were collected from bottles by using a 5 ml plastic syringe (through Teflon seals) and filtered through a 0.22 μ m filter (VWR Labshop) to remove cellular proteins. Then 1 ml filtered samples were analyzed by using method describe above. Wheat protein degradation was estimated by the difference in total protein content in bottle fed with WBF (extracellular protein + wheat protein residue) and in PSBF/MSBF/blank bottles, where only secreted extracellular protein but no wheat protein were present.

2.4.3.7 Determination of Structural Carbohydrates and Lignin Content

The carbohydrates and lignin content in cardboard was analyzed according to NREL standard methods [45, 90]. Before the assay the filtering crucibles were prepared by placing them in a muffle furnace at 575 + 25 °C for at least 4 h to ash to constant weight.

TS in the sample was determined by the method in Sect. 2.4.3.1; at the same time 300 mg air-dried samples were transferred to pressure tubes, then 3 ml 72 % H₂SO₄ was added to each and mixed. Then pressure tubes were incubated in water bath at 30 ± 3 °C for 60 min; every 10–15 min, samples were stirred to ensure a

uniform hydrolysis. After this, the H_2SO_4 was diluted to 4 % by adding 84 ml diH_2O ; the tubes were capped with Teflon screw caps and placed in an autoclave at 121 °C for 1 h. After cooling, the hydrolysis solution was vacuum-filtered through the pre-weighed filtering crucible; filtrates were collected for analysis of the acid-soluble lignin and the carbohydrates contents.

All remaining solids were transferred into filtering crucibles and rinsed with more than 50 ml diH_2O . The crucible and acid-insoluble residues were dried at 105 ± 3 °C for 24 h until a constant weight and after recording the weight, the crucible and residue were transferred into the muffle furnace at 575 ± 25 °C for 48 h until achieving constant weight; then crucible and residue were removed to a dessicator to cool down, and the weights were recorded.

Approx 20 mls of the filtrates were transferred into a flask and neutralized by adding $CaCO_3$. Then samples were then centrifuged twice at 13,000 rpm for 15 min. Approx 1 ml of supernants was transferred to vials and analyzed by HPLC (Agilent Technologies 1,200 series) with a Bio-Rad Aminex HPX-87H column at 50 °C with water as the mobile phase and a flow rate of 0.6 ml/min. Carbohydrate compositions were determined by running against standards for glucose, xylose, galactose, arabinose, and mannose.

Approx 2.5 ml of filtrate was also transferred into a cuvette and acid-soluble lignin was determined by running against a blank sample of diH_2O on the UV-Visible Spectrophotometer (LightwaveII, Biochrom Ltd) at a wavelength of 330 nm. This wavelength and absorptivity constant ϵ (9.1642 L/g-cm) for acid-soluble lignin contained in cardboard were derived from another PhD study at our laboratories [101]. If necessary, the samples were diluted to bring absorbance within the absorbance range 0.7–1.0.

All the samples were performed in five replicates; filter paper (>98 % of cellulose) was used as an internal standard to control for the sugar recovery rate in the hydrolysis; standard sugars were also running through the autoclave hydrolysis procedure with 4 % H_2SO_4 to correct for losses due to degradation during dilute acid hydrolysis.

The carbohydrates and lignin content were calculated based on the following equations

$$ASL = \frac{UV_{abs} \times V_{filtrate} \times Dilution}{\epsilon \times ODW_{sample}} \quad (2.12)$$

$$ODW_{sample} = \frac{Weight_{airdrysample} \times TS\%}{100} \quad (2.13)$$

$$AIL\% = \frac{(Weight_{crucibleplusair} - Weight_{crucible}) - (Weight_{crucibleplusash} - Weight_{crucible})}{ODW_{sample}} \times 100\% \quad (2.14)$$

$$C_{corsample} = \frac{C_{HLPLC}}{\%R_{avesugar}/100} \quad (2.15)$$

$$\%sugar = \frac{C_{corsample} \times Anhydrocorrection \times V_{filtrate} \times \frac{1g}{1000mg}}{ODW_{sample}} \times 100 \quad (2.16)$$

where: Eq. 2.12 is for calculation of acid-soluble lignin (ASL); UV_{abs} is the average UV–Vis absorbance for the sample; $V_{filtrate}$ is the volume of filtrate 87 ml; ε is the absorptivity constant of acid-soluble lignin contained in cardboard 9.1462 L/g-cm [101]; dilution = (Volume_{sample} + Volume_{diluting solvent})/Volume_{sample}, here equals to 1; ODW_{sample} refers to as the dry weight of sample which is calculated from Eq. 2.13. Equation 2.14 is for estimation of acid-insoluble lignin percentage (AIL %); weight_{crucible plus air} is the oven-dried weight of crucible and acid-insoluble residue; Weight_{crucible plus ash} is the ignited weight of crucible and ash.

Equations 2.15 and 2.16 were applied to calculate polymeric sugar content in cardboard. $C_{corsample}$ and C_{HPLC} refer to corrected sugar concentration and sugar content obtained from HPLC respectively; $\%R_{avesugar}$ is the average recovery rate for a specified sugar standard, which is obtained by the ratio of HPLC-detected sugar concentration to the known sugar concentration. $\%sugar$ is the percentage of each sugar as received based; Anhydro-correction is to convert to the concentration of polymeric sugars from the corresponding sugar monomer, anhydro corrections for C-5 sugars (xylose, arabinose) are 0.88 (132/150) and for C-6 sugars (glucose, galactose, and mannose) are 0.90 (162/180).

2.4.4 Statistical Methods

A non-parametric test method—one-tailed Mann–Whitney test was performed on each set of BMP results for different substrates to determine the substrate(s) with greatest biodegradability in AD over the digestion period. All the data were analyzed in Matlab (Matlab R2007b) at significance level $\alpha = 0.05$.

2.5 Composition and Properties of Materials Studied

Data on composition and properties of the products modelled especially the novel materials was not available. Therefore, it was necessary to characterize the composition of modelled products by laboratory research to ensure the important components present in the materials studied were accounted for in LCA model.

As defined in Sect. 2.1.2.2, the raw materials concerned in the modelled product systems (coolbox, display board, and construction concept products) were mainly WBF, potato/maize starch-based foams and cardboard. Their physical–chemical parameters were analyzed using the methods indicated in Sect. 2.4, and are presented below.

2.5.1 Composition of Product Systems

WBF, potato and maize starch based foam were collected from different batches of production representing the foams produced at Greenlight Ltd over the period of Aug 2006–Feb 2009. The cardboard box produced in The Box Factory Ltd in 2007 was used to simulate the cardboard component of coolbox (Hydropac Ltd, product code: CUIB001). The composition of different materials reported by manufacturers and their applications is given in Table 2.2. Moisture and protein contents in wheat flour and moisture contained in starch were derived from manufacturers (Heygates Ltd, Roquete France and Novidon), whereas the moisture content of PVOH feedstock was determined in the laboratory.

2.5.2 Characterisation of Materials

The foams and cardboard collected was kept at 4 °C to be prepared for experimental work. The properties of these materials were analyzed according to the methodology described in Sect. 2.4. Before analysis, the test material was kept spread out at room temperature for 2–3 days and turned once per day to ensure even air-drying until the change in weight was less than 1 % in 24 h. Then the samples were fed into a cutter mill until the entire sample was milled and passed a 10-mesh sieve. All the milled and sieved samples were homogenized and analyzed immediately.

The physico-chemical properties of WBF, cardboard and two additional starch-based foams including the TS, VS, total protein, total N and COD etc., are presented in Table 2.3.

2.5.2.1 TS/VS

VS/TS ratios for all three foams are over 99 %, which indicates a trace amount of inorganic material present in the foams; whereas the cardboard contain higher levels of inorganic material (lower VS/TS). The VS/TS results for cardboard (0.895) in this study are close to the data revealed by a study [94] (0.847) and the Phyllis database [24] (VS/TS = 0.932) but differed from the results reported by Owens and Chynoweth [76] (VS/TS = 0.977) and by Jokela et al. [53] (VS/TS = 0.77).

2.5.2.2 Total N and Total Protein Content

Normally wheat flour contains 10–15 % of protein (based on dry weight); approximately 80 % of the endosperm protein is comprised of gluten including monomeric gliadins and polymeric glutenin (both soluble in SDS) [23, 43]. The

Table 2.2 Composition of materials

	Composition (% w/w)	Data source	LCA case studies			
			Cool box	Display board	Trough mould	Void former
WBF	86.26 % wheat flour (9.5 % protein; moisture 14 %) 13.32 % PVOH (moisture 3.78 %) 0.29 % soy oil Trace amount soy flour	Greenlight Products Ltd Heygates	✓	✓	✓	✓
PSBF	87.23 % potato starch (Moisture 20 %) 12.35 % PVOH (moisture 3.78 %) 0.02 % talc 0.4 % soy oil Trace amount soy flour	Greenlight Products Ltd Roquete Ltd Novidon Ltd.	✓	✓	✓	✓
MSBF	89.64 % maize starch (Moisture 13 %) 9.73 % PVOH (moisture 3.78 %) 0.09 % talc 0.54 % soy oil Trace amount soy flour	Greenlight Products Ltd Roquete Ltd	✓	✓	✓	✓
Cardboard	34.8 % kraftliner (virgin paper based) 30.4 % Wellenstoff (recycled paper based) 34.8 % testliner (recycled paper based)	The Box Factory Ltd Hydropac Ltd	✓			

remaining 20 % is albumins (soluble in water or dilute salty solution) and globulins (soluble in dilute salty solution but not water) [23, 43]. The protein contents were determined with two methods—the Lowry microassay [78] and the TN/protein conversion method i.e. the protein concentration is obtained by multiplying its total N by a nitrogen to protein conversion factor which is calculated from the amino acids composition [72].

In this study the method to determine total N was persulphate digestion, which was developed as an alternative to the Kjeldahl method [19]. The main difference between Kjeldahl and persulphate digestion is that the former can determine organic N and $\text{NH}_4^+\text{-N}$ (not N from NO_2^- and NO_3^-) whereas the latter can convert all forms of N (organic N, and $\text{NH}_4^+/\text{NO}_2^-/\text{NO}_3^-\text{-N}$) to $\text{NO}_3^-\text{-N}$ [19, 92]. Persulphate digestion has been widely applied to water and plant material [81, 91, 92]. The results from previous studies indicate that persulphate digestion is an accurate and precise method for analyzing plant material—N recovery was complete and agreed with Kjeldahl and the results showed lower variability than Kjeldahl [81, 91]. Therefore, results obtained from persulphate digestion (within

Table 2.3 Physical and chemical properties of materials (SD is indicated in brackets)

	WBF	PSBF	MSBF	Cardboard
Gravimetric tests				
TS (%)	93.30 (0.766)	92.72 (0.264)	93.18 (0.188)	95.79 (0.321)
VS (% of TS)	99.10 (0.238)	99.55 (0.057)	99.87 (0.122)	89.46 (0.037)
Ash (% of TS)	0.90	0.45	0.13	10.54
COD test				
COD (mgO ₂ /g TS)	1187.96 (172.67)	1167.26 (251.573)	1252.62 (448.674)	1133.47 (137.117)
COD (mgO ₂ /g VS)	1198.75 (174.245)	1172.5 (252.703)	1254.20 (449.214)	1267.01 (153.273)
Total protein				
mg/g TS	42.55 (6.831)	3.30 (0.551)	4.23 (0.588)	0.00
% of COD	5.37	0.43	0.51	0.00
Total N				
mg/g TS	13.72 (1.519)	0.00	0.00	2.23 (0.0474)
Total S				
SI 181.975 (mg/g TS)	0.90 (0.032)	0.00	0.00	0.76 (0.011)
SI 180.669 (mg/g TS)	0.94 (0.033)	0.00	0.00	0.93 (0.019)
SI 182.563 (mg/g TS)	0.88 (0.031)	0.00	0.00	0.59 (0.009)
Structural carbohydrates and lignin content (% of dry weight)				
Glucose	—	—	—	65.84 (0.963)
Xylose	—	—	—	10.04 (0.329)
Galactose	—	—	—	2.34 (0.099)
Arabinose	—	—	—	0.385 (0.048)
Mannose	—	—	—	6.09 (0.163)
Acid-soluble lignin	—	—	—	1.74 (0.223)
Acid-insoluble lignin	—	—	—	11.26 (0.835)

detection limits) in this study were considered as representative of total N contained in the material for N balance calculations in the LCA model.

The total N results for WBF obtained in this study, 1.37 % of WBF (equivalent to 1.59 % of wheat flour), were close to the results reported in previous studies for wheat grain (1.92 % of TS) [95] and wheat flour (1.63–2.07 % of TS) [4]. Total N contained in the cardboard was determined as 0.223 % of TS, which is higher than the 0.04 % TS found by Jokela et al. [53] but close to other values reported in the literature [30, 94] and the value of 0.25 % of TS cited in the Phyllis database [24].

When converting total N content of WBF to total protein, two Nitrogen Factor (NF) recommended in previous studies were compared—5.7, a recommended NF for wheat grain [4, 36, 72, 95] and 5.52, a proposed NF for wheat flour [69, 86]. In this research, NF 5.52 was applied to WBF due to wheat flour being the main component of WBF. Using this NF, the converted protein from Eq. 2.17 is 75.7 mg/g TS, which gives a higher value than the Lowry microassay result (42.55 mg protein/g TS). This can be partly explained by a non-protein N fraction

present in the total N results [69], such as free amino acids, amides, and other non-polymeric N constituents [47]. However, the non-protein N fraction in wheat is reported to be negligible, only accounting for 1.5 % of total N [47]. Therefore, another factor may be the main reason for the difference between two results. Starch contained in the WBF is a potential interfering substance in the Folin phenol method [77]. Technically, the limitations in methodology could be rectified. For instance, in the persulphate digestion method, inaccuracy caused by non-protein N could be overcome either by determining non-protein N content or extracting protein before N determination [55, 58]; eliminating interfering substances in the protein assay, DOC-TCA precipitation sep suggested by Peterson [77] could be modified (DOC-TCA precipitation may not applicable to wheat proteins). However, considering that the main objective is to determine the total N content in foam/cardboard for N balance in the LCA model, the methodological modifications for protein content determinations were beyond the current scope of this work and were not explored further.

$$\%Protein = \%Nitrogen \times NF \quad (2.17)$$

where: NF = nitrogen factor.

The trace amount of protein content in the MSBF or PSBF could be explained by the protein contained in soy flour—a previous study reported the protein content in soy flour as typically 50 % (within the range of 51–53 % over an 8-year study period) [79]. The soy protein might be introduced into foams via the trace amount of soy flour used as material to lubricate equipment during the foam production process. But the total N content did not confirm the protein assay results. The detection limit for persulphate digestion (detection range 10–150 mgN/L) and Peterson's modified Lowry assay (detection range above 5 mg/L) could cause this error. Converting protein to total N based on Eq. 2.17 (the NF of soybean or meal 5.5 was applied) [69], 0.6 and 0.77 mg N/g TS for PSBF and MSBF were obtained and thus these trace amounts of N were considered as negligible in the N balance calculation for the LCA model.

2.5.2.3 Total COD

In addition to total nitrogen and protein measurement, a total COD test was carried out to analyze the stoichiometric CH_4 potential. The measured COD/TS ratio for foams is between 1.16 and 1.25 g O_2 /g TS, which is close to the calculated theoretical COD value converted from the starch $(C_6H_{10}O_5)_n$ and PVOH $(C_2H_4O)_n$ components in the foams. Here WBF is given as an example to illustrate the calculation carried out based on Eq. 2.18 [96]. Equivalent COD for starch and PVOH are 1.185 and 1.818 g COD/g respectively. As the formula of the protein detected in WBF was not determined, the percentage of COD represented by protein was estimated by assuming a stoichiometric conversion factor of 1.5 which was derived from the protein formula $C_{16}H_{24}O_5N_4$ presented by Rittmann and McCarty [84] and

used to represent solid protein of kitchen waste in a previous study [68]. Therefore, based on the compositions listed in Table 2.2 the calculated equivalent COD for WBF is 1.3 g/g TS, which is consistent with the experimental results.

For the formula $C_nH_aO_bN_c$ (1 mol)

$$\text{COD} = \frac{2 \times n + (a - 3 \times c)/2 - b}{2} \times 32 \text{ g O}_2 \quad (2.18)$$

The COD results for WBF and PSBF are quite close whereas MSBF is slightly higher than other two foams. The COD of cardboard is slightly higher than foams on a total VS basis; but, on the basis of fresh sample, COD value of cardboard is very close to or lower than foams. This suggests that similar potential CH_4 yields could be expected from the same amount of dried/fresh cardboard and foams.

2.5.2.4 Total Sulphur Content

Sulphur is taken by the plant from soil and transferred into amino acids and other organic compounds in plant tissue in the form of sulphate [61]. It is component part of amino acids therefore a component of most proteins, taking a part in initiating protein synthesis. In the case of wheat protein, sulphur plays a role in forming wheat protein determining the baking quality of winter wheat. The sulphur sequestered in wheat protein/wood tissue is present in the final products (WBF/cardboard). The S content in bio-based foams and cardboard was analysed according to the methodology described in Sect. 2.4.2.3.

To test the reliability of the S-measurement technique applied, the blank and additional samples were spiked with NaSO_4 standard (final concentrations of standard is 50 ppm S). The recovery rate for three emission lines and different samples are shown in Table 2.4. On three emission lines, the recovery rate for NaSO_4 varied between 100.6 and 105.36 %, depending on the samples. This range is confirmed by Kalra et al. [57], they tested S recovery rate by using the same microwave digestion plus ICP-OES method, and found the recovery for different sulphur sources ranged from 95.5 to 112.9 %; particularly for Na_2SO_4 , recovery rate was 104.8 ± 3.2 – 112.9 ± 1.9 % depending on the amounts added. Soon et al. [93] also tested this method, they indicated that the S value obtained was higher than the certified limits in the case of some plant tissue (the recovery rate varies between 100.41 and 110.62 %). The recovery rate calculated in this study together with the previous studies are good indications of the high accuracy of the technique used for S element determination.

The S content determined by three emission lines of ICP-OES varied between 0.88 and 0.94 mg/g TS for WBF and between 0.55 and 0.86 mg/g TS for cardboard (see Table 2.3). The result measured by emission line S I 180.669 nm was preferred as it was recommended as more sensitive line [33, 60] and it showed no interference from calcium (SI 181.979 nm has spectral overlap of S and Ca).

Table 2.4 Recovery of S element (SD is indicated in bracket)

NaSO ₄ added as spike				
Emission lines	Amount added (mg/L)	Blank + spike (recovery %)	WBF + spike (recovery %)	Cardboard + spike (recovery %)
SI 181.975 (mg/g TS)	50	100.82 (6.92)	101.79 (0.36)	101.60 (2.90)
SI 180.669 (mg/g TS)	50	105.36 (6.23)	104.06 (4.53)	102.31 (2.59)
SI 182.563 (mg/g TS)	50	100.60 (7.48)	102.33 (0.47)	102.64 (3.04)

Comparing the reading from S I 180.669 emission line with the sulphur content observed in other studies, 0.094 % of WBF is lower than the data reported by Soon et al. [93], Kalra et al. [57]. According to these two previous studies, S accounts for 0.235 % [93] and 0.186 % [57] of wheat flour (oven dry basis), which is equivalent to 0.203 and 0.160 % of WBF respectively (calculation based on 86.26 % of wheat flour component in WBF). For S content in cardboard, the result revealed here (0.093 % of oven dry basis) is slightly lower than the results recorded in Phyllis database (0.12 % of dry wt) [24].

Based on the discussion above, 0.94 mg S/g WBF and 0.93 mg S/g cardboard (dry basis) were used in the LCA to calculate the downstream release of this S during subsequent processing, product use and final disposal stages of the life cycle.

2.5.2.5 Structural Carbohydrates and Lignin Content of Cardboard

As presented in Table 2.3, approx 84.7 % of oven-dried weight corresponded to polysaccharides, this result is higher than the carbohydrate content of cardboard reported by Yáñez et al. [106] (75 % polysaccharides).

Amongst all the polymeric sugar contained in cardboard, glucan was main component, accounting for 65.8 % of the mass. This result is consistent with studies by Shi et al. [87] that 64.1 % of the dry weight of mixed paper and 48.8 % of cardboard was glucan, and Yáñez et al. [106], who reported 59.7 % of cellulose content in cardboard.

Hemicelluloses are the second most abundant polysaccharide types in the plant cell wall, usually constituting about 20–35 % of the mass [87]. Hemicellulose (including xylan, galactan, mannan, araban) accounted for 18.86 % of the mass of oven-dried cardboard in the present study. Xylan was the major monomer (10 % of oven-dry basis), close to the 8.5 % reported by Shi et al. [87]. Conversely, in the current study other sugars contained in hemicellulose were not negligible with 6 % mannan and 2.3 % galactan. Yáñez et al. [106] and Barlaz et al. [5] reported 13.8 and 9.9 % hemicellulose content respectively- somewhat lower than the hemicellulose content in the cardboard in the present study.

After dilute acid hydrolysis, part of the lignin was soluble in H₂SO₄ but most was acid-insoluble accounting for over 11 % of the oven-dry mass of cardboard,

which is consistent with previous studies [87, 106], their results fell into the range 14–15 % of acid-insoluble lignin content (oven-dry basis).

All the test results presented here were corrected for the recovery rate of standard sugars or filter paper. If the recovery rate of glucose is disregarded then the average conversion efficiency of cellulose contained in filter paper was 99.2 %; if the recovery rate was included then the efficiency was quantified as 104 %. This indicated that the two-step acid hydrolysis was thorough and efficient. Therefore, it could be assumed that nearly 100 % of the polymeric sugars contained in cardboard were hydrolyzed to sugar monomer.

Based on the compositional analysis, it was estimated that C component sequestered from atmosphere during wood growing and present in cardboard was 45.84 % on oven-dry basis, which is equivalent to 1.68 kg CO₂/kg oven-dried cardboard. Where the C content in polymeric sugar was calculated from their molar mass; C contained in lignin fraction was estimated as 62.2 % oven dry basis, which was derived from the softwood composition in the Phyllis database [24]. The reason for choosing softwood data is the raw wood logs/saw mill residues used for paper making are primarily derived from softwood, accounting for 71 %, especially for kraftliner which is the main component of facing for the cardboard under analysis and 81.5 % of the feedstocks are softwood [25]. This C content obtained from laboratory test was used in the LCA model to track the fate of C over the life cycle of the cardboard component contained in coolbox.

References

1. Althaus H-J, Doka G, Dones R, Heck T, Hellweg S, Hirschier R, Nemecek T, Rebitzer AG, Spielmann M (2004) Overview and methodology
2. Angelidaki I, Alves M, Bolzonella D, Borzacconim L, Guwy AJ, Kalyuzhnyi S, Jenicek P, Campos L, Van Ier JB (2008) Defining the biomethane potential (BMP) of solid organic wastes: a proposed protocol for batch assays. In: 5th International symposium of anaerobic digestion of solid waste and energy crops, Hammamet, Tunisia
3. APHA (1999) Standard methods for the examination of water and wastewater. American Public Health Association, Washington
4. Barikmo I, Ouattara F, Oshaug A (2003) Protein, carbohydrate and fibre in cereals from mali—how to fit the results in a food composition table and database. In: 5th International food data conference/27th national nutrient databank conference, Jun 30–Jul 03 2003. Academic Press Inc Elsevier Science, Washington, pp 291–300
5. Barlaz MA, Eleazer WE, Odle WS, Qian IX, Wang Y-S (1997) Biodegradative analysis of municipal solid waste in laboratory-scale landfills, EPA
6. Baumgartner CE (1987) Spectrophotometric determination of poly(vinyl alcohol) in cadmium hydroxide pastes. *Anal Chem* 59:2716–2718
7. Bellamy PH, Loveland PJ, Bradley RI, Lark RM, Kirk GJD (2005) Carbon losses from all soils across England and Wales 1978–2003. *Nature* 437:245–248
8. Benson J, Fleishman JA (1994) The robustness of maximum-likelihood and distribution-free estimators to nonnormality in confirmatory factor-analysis. *Qual Quant* 28:117–136
9. Björklund A (2002) Survey of approaches to improve reliability in LCA. *Int J Life Cycle Assess* 7:64–72

10. Boustead I (2005a) Eco-profiles of the european plastics industry. Pastics Europe (association of plastics manufacturers)
11. Boustead I (2005b) Eco-profiles of the European plastics industry—methodology. In: Manufacturers AOP Plastic Europe
12. Brown L, Armstrong Brown S, Jarvis SC, Syed B, Goulding KWT, Phillips VR, Sneath RW, Pain BF (2001) An inventory of nitrous oxide emissions from agriculture in the UK using the IPCC methodology: emission estimate, uncertainty and sensitivity analysis. *Atmos Environ* 35:1439–1449
13. Brown L, Syed B, Jarvis SC, Sneath RW, Phillips VR, Goulding KWT, Li C (2002) Development and application of a mechanistic model to estimate emission of nitrous oxide from UK agriculture. *Atmos Environ* 36:917–928
14. BSI (2008) PAS 2050: 2008 Specification for the assessment of the life cycle greenhouse gas emissions of goods and services. In: Standards B (ed) BSI
15. CEH (2006) UK deposition maps. Centre Ecol Hydro
16. CEH (2009) UK pollution and deposition. Center Ecol Hydro
17. Cordek (2009a) Formwork solutions [Online]. Available: <http://www.cordek.com/docs/Formwork%20Solutions%20Brochure%20-%20April%202007.pdf>. Accessed 25 Oct 2009
18. Cordek (2009b) *Trough moulds for in situ ribbed floors* [Online]. Available: <http://cordek.com/docs/New%20Trough%20Brochure%20-%20final!.pdf>. Accessed 25 Oct 2009
19. Delia CF, Steudler PA, Corwin N (1977) Determination of total nitrogen in aqueous samples using persulfate digestion. *Limnol Oceanogr* 22:760–764
20. Derwent RG, Jenkin ME, Saunders SM (1996) Photochemical ozone creation potentials for a large number of reactive hydrocarbons under European conditions. *Atmos Environ* 30:181–199
21. Derwent RG, Jenkin ME, Saunders SM, Pilling MJ (1998) Photochemical ozone creation potentials for organic compounds in northwest Europe calculated with a master chemical mechanism. *Atmos Environ* 32:2429–2441
22. DTI (2007) Energy and commodity balances, conversion factors and calorific values. DTI
23. Dupont FA, Samoil V, Chan R (2008) Extraction of up to 95 % of wheat (*Triticum aestivum*) flour protein using warm sodium dodecyl sulfate (SDS) without reduction or sonication. *J Agri Food Chem* 56:7431–7438
24. ECN (2007) Phyllis, database for biomass and waste. Energy research Centre of the Netherlands
25. Fefco GE (2006) European database for corrugated board life cycle studies
26. Finch CA (1992) Polyvinyl alcohol-developments. Wiley, Chichester
27. Finnveden G, Hauschild MZ, Ekvall T, Guinee J, Heijungs R, Hellweg S, Koehler A, Pennington D, Suh S (2009) Recent developments in life cycle assessment. *J Environ Manage* 91:1–21
28. Folland CK, Karl TR, Christy JR, Clarke RA, Gruza GV, Jouzel J, Mann ME, Oerlemans J, Salinger MJ, Wang S-W (2001) Climate change 2001: the scientific basis. contribution of working group I to the third assessment report of the intergovernmental panel on climate change. In: Houghton JT, Ding Y, Griggs DJ, Noguer M, Van der Linden PJ, Dai X, Maskell K, Johnson CA (ed) Cambridge University Press, Cambridge, United Kingdom and New York
29. Forster P, Ramaswamy V, Artaxo P, Bernsten T, Betts R, Fahey D W, Haywood J, Lean J, Lowe DC, Myhre G, Nganga J, Prinn R, Raga G, Schulz M, Dorland RV (2007) Changes in atmospheric constituents and in radiative forcing. In: Climate change 2007: the physical science basis. Contribution of working group I to the fourth assessment report of the intergovernmental panel on climate change. Cambridge University Press, Cambridge, United Kingdom and New York
30. Francou C, Lineres M, Derenne S, Le Villio-Poitrenaud M, Houot S (2008) Influence of green waste, biowaste and paper-cardboard initial ratios on organic matter transformations during composting. *Bioresour Technol* 99:8926–8934

31. Frischknecht R, Jungbluth N, Althaus H-J, Doka G, Heck T, Hellweg S, Hirschier R, Nemecek T, Rebitzer G, Spielmann M, Wernet G (2007) Overview and methodology ecoinvent report No.1: swiss center for life cycle inventories, Dubendorf
32. Goulding K (2008) Atmospheric CO₂ and NH₃ concentration for modeling work. Personal communication, London
33. Grosser ZA, Davidowski LJ, Wee P (2009) The analysis of biodiesel for inorganic contaminants including sulfur by ICP-OES
34. Guinée JB, Gorree M, Heijungs R, Huppes G, Kleijn R, Koning A, Oers LV, Sleeswijk AW, Suh S, Haes HAU, Bruijn H, Duin RV, Huijbregts MAJ (2001). Life cycle assessment an operational guide to the ISO standards final report (part 1, 2, 3). Ministry of housing, spatial planning and the environment and center of environmental science, Leiden University
35. Hafez AA, Goyal SS, Rains DW (1991) Quantative determination of total sulphur in plant tissue using acid digestion and ion-chromatography. *Agri J* 83:148–153
36. Hames B, Scarlata C, Sluiter A (2005) Laboratory analytical procedure (LAP) determination of protein content in biomass national renewable energy laboratory
37. Heijungs R, Guinée J, Kleijn R, Rovers V (2007) Bias in normalization: causes, consequences, detection and remedies. *Int J Life Cycle Assess* 12:211–216
38. Heijungs R, Guinée JB, Huppes G, Lankreijer RM, Udo de Haes HA, Wegener Sleeswijk A, Ansems AMM, Eggels PG, Duin RV, Goede HPD (1992) Environmental life cycle assessment of products guide and backgrounds leiden: center of environmental science
39. Huijbregts MA (1999) Priority assessment of toxic substances in the frame of LCA-development and application of the multi-media fate, exposure and effect model USES-LCA. Interfaculty department of environmental science faculty of environmental sciences. University of Amsterdam, Amsterdam
40. Huijbregts MAJ, Breedveld L, Huppes G, de Koning A, van Oers L, Suh S (2003) Normalisation figures for environmental life-cycle assessment: The Netherlands (1997/1998), Western Europe (1995) and the world (1990 and 1995). *J Cleaner Prod* 11:737–748
41. Huijbregts MAJ, Norris G, Bretz R, Ciroth A, Maurice B, von Bahr B, Weidema B, de Beaufort ASH (2001) Framework for modelling data uncertainty in life cycle inventories. *Int J Life Cycle Assess* 6:127–132
42. Huijbregts MAJ, Thissen U, Guinée JB, Jager T, Kalf D, van de Meent D, Ragas AMJ, Sleeswijk AW, Reijnders L (2000) Priority assessment of toxic substances in life cycle assessment. Part I: calculation of toxicity potentials for 181 substances with the nested multi-media fate, exposure and effects model USES-LCA. *Chemosphere* 41:541–573
43. Hurkman WJ, Tanaka CK (2007) Extraction of wheat endosperm proteins for proteome analysis. *J Chromatogr B-Anal Technol Biomed Life Sci* 849:344–350
44. Hutchinson JJ, Grant BB, Smith WN, Desjardins RL, Campbell CA, Worth DE, Verge XP (2006) Estimates of direct nitrous oxide emissions from Canadian agroecosystems and their uncertainties. *Can J Soil Sci*
45. Hyman D, Sluiter A, Crocker D, Johnson D, Sluiter J, Black S, Scarlata C (2007) Determination of acid soluble lignin concentration curve by UV-Vis spectroscopy laboratory analytical procedure (LAP)
46. IIASA (2007) Regional air pollution information and simulation model. *Int Inst Appl Syst Anal*
47. Imafidon GI, Sosulski FW (1990) Nonprotein nitrogen contents of animal and plant foods. *J Agri Food Chem* 38:114–118
48. IPCC (2006) 2006 IPCC guidelines for national greenhouse gas inventories In: Eggleston HS, Buendia L, Miwa K, Ngara T, Tanabe K (ed) National greenhouse gas inventories programme
49. ISO (1998) ISO 14041 environmental management—life cycle assessment—goal and scope definition and inventory analysis. In: Standardization IOF (ed) British standards institution
50. ISO (2000a) ISO 14042 environmental management—life cycle assessment—life cycle impact assessment

51. ISO (2000b) ISO 14049 Environmental Management—Life Cycle Assessment—Examples of Application of ISO 14041 to goal and scope definition and inventory analysis. British Standards Institution, London, UK
52. Jenkin ME, Hayman GD (1999) Photochemical ozone creation potentials for oxygenated volatile organic compounds: sensitivity to variations in kinetic and mechanistic parameters. *Atmos Environ* 33:1275–1293
53. Jokela JPY, Vavilin VA, Rintala JA (2005) Hydrolysis rates, methane production and nitrogen solubilisation of grey waste components during anaerobic degradation. *Bioresour Technol* 96:501–508
54. Joshi DP, Lanchunfung YL, Pritchard JG (1979) Determination of polyvinyl-alcohol via its complex with boric-acid and iodine. *Anal Chim Acta* 104:153–160
55. Jung S, Rickert DA, Deak NA, Aldin ED, Recknor J, Johnson LA, Murphy PA (2003) Comparison of kjeldahl and dumas methods for determining protein contents of soybean products. *J Am Oil Chem Soc* 80:1169–1173
56. Jungmeier G, Werner F, Jarnehammar A, Hohenthal C, Richter K (2002) Allocation in LCA of wood-based products—experiences of cost action E9 part I. Methodology. *Int J Life Cycle Assess* 7:290–294
57. Kalra YP, Maynard DG, Radford FG (1989) Microwave digestion of tree foliage for multi-element analysis. *Can J For Res-Revue Canadienne De Recherche Forestiere* 19:981–985
58. Kamizake NKK, Goncalves MM, Zaia C, Zaia DAM (2003) Determination of total proteins in cow milk powder samples: a comparative study between the Kjeldahl method and spectrophotometric methods. *J Food Compos Anal* 16:507–516
59. Kennedy D, Montgomery D, Rollier D, Keats J (1997) Data quality. *Int J Life Cycle Assess* 2:229–239
60. Kola H, Perämäkia P, Välimäki I (2002) Correction of spectral interference of calcium in sulfur determination by inductively coupled plasma optical emission spectrometry using multiple linear regression. *J Anal At Spectrom* 17:5
61. Kovacs AB, Prokisch J, Kovacs B, Palencsar AJ, Gyori Z, Loch J (1999) Determination of sulphur in plant extracts by ion chromatograph—hydraulic high-pressure nebulizer Inductively coupled plasma atomic emission spectrometer (IC/HPN/ICP-AES). *Int Symp Soil Plant Anal*, 22–26 Mar 1999. Marcel Dekker Inc, Brisbane, pp 1941–1948
62. Li C, Zhuang Y, Cao M, Crill P, Dai Z, Frolking S, Moore B, Salas W, Song W, Wang X (2001) Comparing a process-based agro-ecosystem model to the IPCC methodology for developing a national inventory of N₂O emissions from arable lands in China. *Nutr Cycl Agroecosyst* 60:159–175
63. Li CS (2000) Modeling trace gas emissions from agricultural ecosystems. *Nutr Cycl Agroecosyst* 58:259–276
64. Li CS, Farahbakhshazad N, Jaynes DB, Dinnes DL, Salas W, McLaughlin D (2006) Modeling nitrate leaching with a biogeochemical model modified based on observations in a row-crop field in Iowa. *Ecol Model* 196:116–130
65. Li CS, Frolking S, Frolking TA (1992) A model of nitrous-oxide evolution from soil driven by rainfall events. 1. Model structure and sensitivity. *J Geophys Res-Atmos* 97:9759–9776
66. Li CS, Frolking S, Harriss R (1994) Modeling carbon biogeochemistry in agricultural soils. *Global Biogeochem Cycles* 8:237–254
67. Li CS, Mosier A, Wassmann R, Cai Z, Zheng X, Huang Y, Tsuruta H, Boonjawat J, Lantin R (2004) Modeling greenhouse gas emissions from rice-based production systems: sensitivity and upscaling. *Global Biogeochem Cycles* 18:GB1043
68. Li S-L, Kuo S-C, Lin J-S, Lee Z-K, Wang Y-H, Cheng S-S (2008) Process performance evaluation of intermittent-continuous stirred tank reactor for anaerobic hydrogen fermentation with kitchen waste. *Int J Hydrogen Energy* 33:1522–1531
69. Mariotti F, Tome D, Mirand PP (2008) Converting nitrogen into protein—beyond 6.25 and Jones' factors. *Crit Rev Food Sci Nutr* 48:177–184
70. Ministry of Agriculture FAF (1986) The analysis of agricultural materials London, Her majesty's stationery office

71. Mortimer ND, Elsayed MA, Horne RE (2004) Energy and greenhouse gas emissions for bioethanol production from wheat grain and sugar beet
72. Mosse J (1990) Nitrogen to protein conversion factor for 10 cereals and 6 legumes or oilseeds—a reappraisal of its definition and determination—variation according to species and to seed protein-content. *J Agri Food Chem* 38:18–24
73. NSRI (2007) The national soil map and soil classification. National Soil Resources Institute of Cranfield University
74. National Soil Resources Institute (NSRI) (2009) Full soils site report for location 579609E, 307801 N, 5 x 5 km, Cranfield University
75. Owen WF, Stuckey DC, Healy JB, Young LY, McCarty PL (1979) Bioassay for monitoring biochemical methane potential and anaerobic toxicity. *Water Res* 13:485–492
76. Owens JM, Chynoweth DP (1993) Biochemical methane potential of municipal solid-Waste (MSW) components. *Water Sci Technol* 27:1–14
77. Peterson G (1983) Determination of total protein. *Methods Enzymol* 91:25
78. Peterson GL (1977) Simplification of protein assay method of lowry et al—which is more generally applicable. *Anal Biochem* 83:346–356
79. Porter MA, Jones AM (2003) Variability in soy flour composition. *J Am Oil Chem Soc* 80:557–562
80. Préconsultants (2004) Simapro 7.0 database manual methods library
81. Purcell LC, King CA (1996) Total nitrogen determination in plant material by persulfate digestion. *Agron J* 88:111–113
82. Raposo F, Banks CJ, Siegert I, Heaven S, Borja R (2006) Influence of inoculum to substrate ratio on the biochemical methane potential of maize in batch tests. *Process Biochem* 41:1444–1450
83. Reay DS, Dentener F, Smith P, Grace J, Feely RA (2008) Global nitrogen deposition and carbon sinks. *Nature Geosci* 1:430–437
84. Rittmann BE, McCarty PL (2001) Environmental biotechnology: principles and applications. McGraw-Hill, London
85. Rosenbaum R, Bachmann T, Gold L, Huijbregts M, Jolliet O, Juraske R, Koehler A, Larsen H, Macleod M, Margni M, McKone T, Payet J, Schuhmacher M, van de Meent D, Hauschild M (2008) USEtox—the UNEP-SETAC toxicity model: recommended characterisation factors for human toxicity and freshwater ecotoxicity in life cycle impact assessment. *Int J Life Cycle Assess* 13:532–546
86. Sarwar G, Christensen DA, Finlayson AJ, Friedman M, Hackler LR, Mackenzie SL, Pellett PL, Tkachuk R (1983) Inter-laboratory and intra-laboratory variation in amino-acid-analysis of food proteins. *J Food Sci* 48:526–531
87. Shi J, Ebrik M, Yang B, Wyman CE (2009) The potential of cellulosic ethanol production from municipal solid waste: a technical and economic evaluation. University of California Energy Institute, California
88. Sluiter A, Hames B, Hyman D, Payne C, Ruiz R, Scarlata C, Sluiter J, Templeton D, Wolfe J (2008) Determination of total solids in biomass and total dissolved solids in liquid process samples. National Renewable Energy Laboratory, Colorado
89. Sluiter A, Hames B, Ruiz R, Scarlata C, Sluiter J, Templeton D (2005) Determination of ash in biomass. National Renewable Energy Laboratory, Colorado
90. Sluiter A, Hames B, Ruiz R, Scarlata C, Sluiter J, Templeton D, Crocker D (2008) Determination of structural carbohydrates and lignin in biomass laboratory analytical procedure. National Renewable Energy Laboratory, Colorado
91. Smart MM, Rada RG, Donnermeyer GN (1983) Determination of total nitrogen in sediments and plants using persulfate digestion—an evaluation and comparison with the kjeldahl procedure. *Water Res* 17:1207–1211
92. Smart MM, Reid FA, Jones JR (1981) A comparison of a persulfate digestion and the kjeldahl procedure for determination of total nitrogen in fresh-water samples. *Water Res* 15:919–921

93. Soon YK, Kalra YP, Abboud SA (1995) Comparison of some methods for the determination of total sulfur in plant tissues. In: 4th International symposium on soil and plant analysis—quality of soil and plant analysis in view of sustainable agriculture and the environment, Aug 05–10 1995, Marcel Dekker Inc, Wageningen, pp 809–818
94. Sørum L, Grønli MG, Hustad JE (2001) Pyrolysis characteristics and kinetics of municipal solid wastes. *Fuel* 80:1217–1227
95. Sosulski FW, Imafidon GI (1990) Amino-acid-composition and nitrogen-to-protein conversion factors for animal and plant foods. *J Agri Food Chem* 38:1351–1356
96. Speece RE (1996) Anaerobic biotechnology for industrial wastewaters. Archae Press, Nashville
97. Sugiyama H, Fukushima Y, Hirao M, Hellweg S, Hungerbühler K (2005) Using standard statistics to consider uncertainty in industry-based life cycle inventory databases. *Int J Life Cycle Assess* 10:399–405
98. Tang YS, Dijk NV, Anderson M, Simmons I, Dore AJ, Dragosits U, Bealey WJ, Leaver D, Smith RI, Sutton MA (2008) Analysis of temporal and spatial patterns of NH₃ and NH₄⁺ over the UK—2007 Annual report to DEFRA
99. USDA (2009) Soil texture calculator [Online]. USDA. Available: <http://soils.usda.gov/technical/aids/investigations/texture/>
100. USEPA (1995) Guidelines for assessing the quality of life cycle inventory analysis. In: Office of solid waste and us environmental protection agency, w
101. Wang L (2009) Wavelength and the absorptivity constant of biomass (L/g-cm) for acid-soluble lignin of cardboard. Personal communication
102. Weidema B (2000) Avoiding co-product allocation in life-cycle assessment. *J Ind Ecol* 4:11–33
103. Weidema BP, Wesnæs MS (1996) Data quality management for life cycle inventories—an example of using data quality indicators. *J Cleaner Prod* 4:167–174
104. Wichmann FA, Hill NJ (2001) The psychometric function: I. Fitting, sampling, and goodness of fit. *Percept Psychophysics* 63:1293–1313
105. WMO (2007) Scientific assessment of ozone depletion: 2006 global ozone research and monitoring project—report No. 50. World Meteorological Organization
106. Yáñez R, Alonso JL, Parajó JC (2004) Production of hemicellulosic sugars and glucose from residual corrugated cardboard. *Process Biochem* 39:1543–1551
107. Zar JH (1999) Biostatistical analysis. Prentice Hall International Inc, Englewood Cliffs
108. Zhao F, McGrath SP, Crosland AR (1994) Comparison of 3 wet digestion methods for the determination of plant sulfur by inductively-coupled plasma-atomic emission-spectroscopy (ICPAES). *Commun Soil Sci Plant Anal* 25:407–418

Life Cycle Assessment (LCA) of Light-Weight
Eco-composites

Guo, M.

2012, XVIII, 404 p., Hardcover

ISBN: 978-3-642-35036-8